Transverse Orientation of Lamellae and Cylinders by Solution Extrusion of a Pentablock Copolymer

Tamotsu Harada, Frank S. Bates, and Timothy P. Lodge*,†

Department of Chemical Engineering & Materials Science, University of Minnesota, Minneapolis, Minnesota 55455-0431

Received April 2, 2003
Revised Manuscript Received June 2, 2003

Introduction. One of the most appealing properties of block copolymer materials is their ability to adopt a rich variety of predictable, equilibrium ordered states.[1−4] In several cases it has proven possible under laboratory conditions to prepare macroscopic "single crystals" of lamellae,[5−10] cylinders,[11−14] gyroid,[15−17] or cubic morphologies.[18−22] Numerous potential applications for such highly organized microstructures have been identified, particularly for the anisotropic phases.[23−25] However, it is fair to say that anisotropic block copolymer attributes such as ionic transport, barrier and membrane properties, and mechanical strength have not yet enjoyed widespread commercial application, due in part to a dearth of flexible and simple processing strategies for achieving desired macroscopic orientations. The laboratory conditions referred to above include primarily large-amplitude oscillatory shear flow,[5−10,13−21] but also thermal annealing,[15,21] roll casting,[11,26−28] and the application of electric fields.[29−31]

In this preliminary report we describe the application of solution extrusion, or "wet spinning", as a rapid and facile means to prepare macroscopic quantities of highly aligned block copolymer microstructures. We demonstrate that two different microstructures (lamellae and cylinders), each with two distinct orientations, can be prepared from a single parent material by varying flow rate and annealing history. Most remarkably, it is possible to generate the transverse lamellar orientation, i.e., with the lamellar normals parallel to the flow direction, by extruding an ABABA pentablock copolymer solution at high shear rates. Interestingly, the corresponding ABA triblock copolymer does not adopt this orientation under any accessible conditions. This contrast highlights the crucial role of chain architecture in the response of copolymer materials to strong flow conditions.

Experimental Section. A poly(styrene-*b*-butadiene-*b*-styrene-*b*-butadiene-*b*-styrene) (SBSBS) pentablock copolymer, and the molecular weight and composition-matched SBS triblock copolymer, were generously provided by the Dow Chemical Co. Both samples had weight-average molecular weights of 1.1×10^5, polydispersity indices less than 1.1, and PB compositions of 30 wt %. The three S blocks in SBSBS were nominally equal in molecular weight. Polymer solutions (55 wt %) were prepared in a 60:40 heptane:toluene mixture. Solutions were extruded through a syringe with orifice length 8 mm, orifice radius $R_{ex} = 1$ mm, and a piston radius $R_p = 7.8$ or 4.5 mm, using a capillary rheometer to control the plunger speed S. Extrudates were solidified either by (i) immediate coagulation in methanol/dry ice, warming to room temperature in methanol overnight, followed by drying in air at room temperature, or (ii) immediate drying in air at room temperature. To assess the state of order after drying, the samples were examined by small-angle X-ray scattering (SAXS) at the University of Minnesota SAXS facility. X-rays ($\lambda = 1.542$ Å) from a Rigaku rotating anode were monochromated and collimated with Franks mirrors, and scattering patterns were collected on a multiwire area detector (Siemens) located 230 cm behind the sample.

Results and Discussion. The undiluted samples adopt the hexagonally packed cylinder morphology (C), whereas the solutions exhibited a lamellar structure (L), as a consequence of the selectivity of the mixed solvent toward the PB blocks. Both polymer concentration and solvent composition exerted a strong influence on the orientational response of the copolymers, but in this report we focus on a single concentration and composition. Figure 1 presents a schematic illustration of the syringe and four possible states of orientation of L in the extrudate. The extrusion direction is denoted z and the radial direction r. When the lamellar normals are parallel to z, the orientation is termed "transverse". On the other hand, if the lamellar normals are orthogonal to z, there are various possibilities as illustrated in Figure 1. These include "circumferential" (normals along r), "radial" (normals orthogonal to r), and "perpendicular" (normals aligned along a single laboratory axis ("x") normal to z). Samples were examined with X-rays incident along z and along r, which is sufficient to distinguish among transverse, circumferential, and perpendicular, but not between circumferential and radial; however, because of the constraint of (approximately) constant lamellar spacing, the radial orientation seems unlikely a priori, at least without a high population of defects.

Flow conditions were characterized by the wall shear rate $\dot{\gamma}$:

$$\dot{\gamma} = \frac{4SR_p^{\,2}}{R_{ex}^{\,3}} \qquad (1)$$

which could be varied between 8 and 1700 s^{-1}. Parts a and b of Figure 2 show the X-ray patterns for coagulated SBSBS samples viewed along the z and r directions, after extrusion at $\dot{\gamma} = 8$ s^{-1} and $\dot{\gamma} = 720$ s^{-1}, respectively. At the lower rate the orientation is some mixture of perpendicular and circumferential, but at the higher rate the orientation is clearly transverse. So far as we are aware, this represents the first observation of a robust route to producing what has been referred to as the "forbidden" orientation of L. Studies as a function of $\dot{\gamma}$ show that the transition to transverse is quite abrupt, occurring between 40 and 70 s^{-1}. Above the transition the degree of alignment improves slightly as $\dot{\gamma}$ is increased, as quantified by the appropriate order parameter. The domain spacing estimated after annealing at 70 °C for 24 h remains roughly constant, at 203 ± 2 Å, but is distinctly larger than the spacing obtained below the transition (195 ± 3 Å). In sharp contrast, the SBS triblock exhibits no such transition in behavior over

---

[†] Also Department of Chemistry, University of Minnesota.
[*] Author for correspondence: e-mail lodge@chem.umn.edu.

10.1021/ma034417b CCC: $25.00

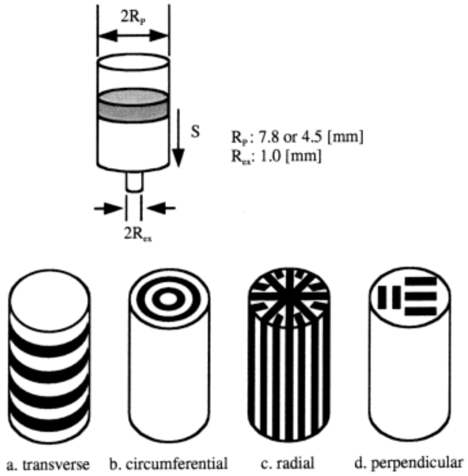

Figure 1. Schematic illustration of the syringe and four possible states of lamellar orientation by solution extrusion with cylindrical die: (a) transverse, (b) circumferential, (c) radial, and (d) orthogonal.

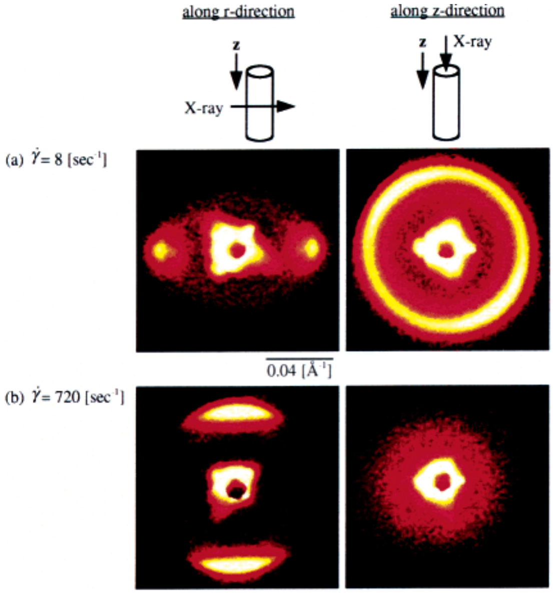

Figure 2. 2D SAXS patterns obtained for coagulated SBSBS samples viewed along the *z* and *r* directions, after extrusion (a) at $\dot{\gamma} = 8$ s^{-1} and (b) at $\dot{\gamma} = 720$ s^{-1}, respectively.

the entire range of accessible shear rates (up to 1700 s^{-1}), underscoring the key role that chain architecture exerts on flow orientation of microdomains. Typical results are shown in Figure 3 for SBS extruded at shear rates of 20 and 1700 s^{-1}.

One possible explanation for these phenomena is that the strong shear extends the SBSBS chains along the flow direction and that the partially aligned chains template the growth of microdomains perpendicular to *z*. The transition from perpendicular to transverse occurs at a Deborah number of around 0.5, based on the onset of shear thinning in shear rheometry. This hypothesis is reminiscent of the shish-kebab morphology observed in crystallization of solution-spun and drawn fibers, where chain extension nucleates order in an orthogonal direction.[32,33] The SBSBS solution is nominally in the L state during shear, so this mechanism may require localized “melting” of misoriented domains. This is also plausible, in that the SBSBS solution is not too far from a lyotropic order–disorder transition; increasing the fraction of the solvent by a few percent (from 40% to 55%) results in the loss of all higher order SAXS peaks. The fact that the lamellar spacing is enhanced in the transverse state is also consistent with some chain extension along the flow direction. In this picture the failure of the triblock to exhibit the same transition might appear surprising, given that the chain length, composition, and concentration is the same, and therefore the stress exerted by the flow on individual chains should be comparable between SBSBS and SBS. However, it is important to note that the block lengths in SBS are roughly double those in SBSBS, so the order–disorder transition is much further away (e.g., solvent fractions greater than 75%); this could suppress the local domain melting.

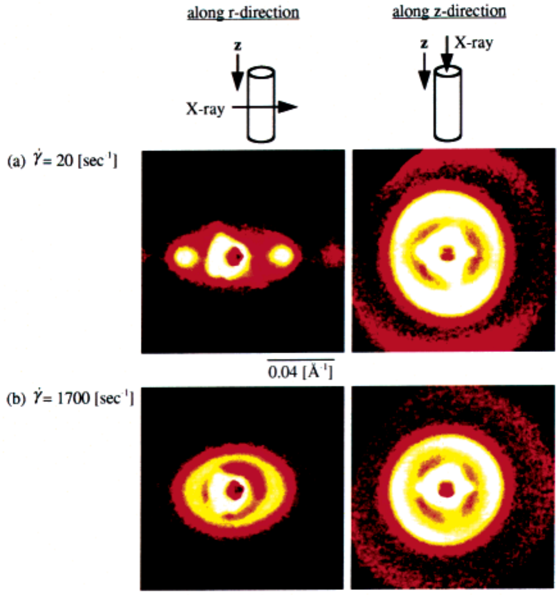

Figure 3. 2D SAXS patterns obtained for coagulated SBS samples viewed along the *z* and *r* directions, after extrusion (a) at $\dot{\gamma} = 20$ s^{-1} and (b) at $\dot{\gamma} = 1700$ s^{-1}, respectively.

An alternative hypothesis rests entirely on the chain architecture difference. In the case of SBS, none of the S domains have bridging blocks, and thus the center planes of each S domain can act as slip planes. In contrast, some significant fraction of center S blocks in SBSBS will bridge the S domains, thereby suppressing slip within the layers. As a consequence, SBSBS prefers the transverse orientation to avoid excessive stretching of the center BSB units, whereas SBS can accommodate any stretching of B by slipping in S. (To some extent, SBSBS could satisfy this constraint by adopting the radial orientation, but as noted above this arrangement has problems of its own.) This argument is supported by the fact that over the regime of shear rate where the transverse orientation appears, the pentablock has a significantly higher viscosity than the triblock, whereas in the Newtonian regime they are similar. It should be noted that these two hypotheses are not mutually exclusive; the first one emphasizes kinetic factors that could facilitate the transverse orientation, whereas the second one is based more on minimizing stress under flow.

After solidification the orientation and nonequilibrium L morphology were maintained by the vitrification of the polystyrene domains. However, the samples converted to C after annealing above T_g. Representative X-ray patterns along the *x*-direction are shown in parts a and b of Figure 4 for the SBSBS samples originally

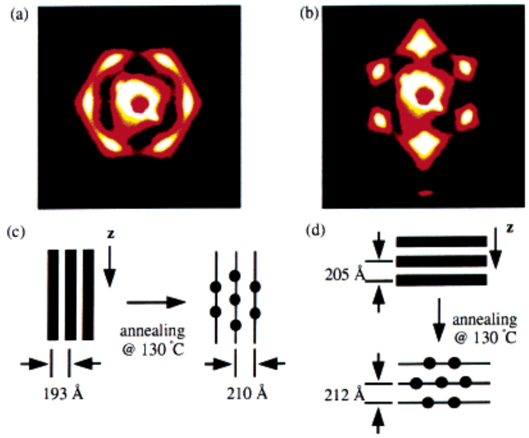

Figure 4. SAXS profiles viewed along r of SBSBS samples after annealing at 130 °C for 24 h: (a) $\dot{\gamma} = 8$ s^{-1} and (b) $\dot{\gamma} = 720$ s^{-1}. Schematic illustration of the transition process from L to H during the thermal annealing: (c) $\dot{\gamma} = 8$ s^{-1} and (d) $\dot{\gamma} = 720$ s^{-1}. The domain spacings of L shown in these illustrations were estimated from the SAXS data obtained for the annealed samples at 70 °C for 24 h.

extruded at 8 and 720 s^{-1}, respectively, but then annealed at 130 °C for 24 h. In both cases highly oriented cylinders emerge, with the cylinder axes primarily transverse to the extrusion direction. However, the orientation of the six-spot pattern reflects an epitaxial relationship with the preceding L phase, as illustrated in Figure 4c,d. The cylinders are more highly aligned when growing from the transverse L, due in part to the greater perfection of a single L orientation and possibly also to a domain spacing match between the lamellar planes and the (100) cylinder planes. In either case, however, it is clear that highly oriented cylindrical phases can be obtained by this route, with orientations that almost certainly could not be produced by direct extrusion in C.

These results serve to introduce a new way to process microstructured block copolymers via solution extrusion and illustrate how a variety of orientations of both lamellae and cylinders can be produced from a single material. Of particular interest is the strong role played by chain architecture, with the pentablock copolymer providing access to the transverse lamellar state. A fuller description of the roles of concentration, solvent composition, flow rate, die geometry, and annealing conditions will be provided subsequently. Furthermore, under some conditions the mechanical properties of the extruded materials can be far superior to those flow oriented by more familiar means.

Acknowledgment. This work was supported in part by the MRSEC Program of the National Science Foundation under Award DMR-0212302. We also acknowledge the support of the Characterization Facility, Institute of Technology, University of Minnesota.

References and Notes

(1) Matsen, M. W.; Bates, F. S. *Macromolecules* **1996**, *29*, 1091−1098.
(2) Bates, F. S.; Fredrickson, G. H. *Phys. Today* **1999**, *52*, 32−38.
(3) Lodge, T. P. *Macromol. Chem. Phys.* **2003**, *204*, 265−273.
(4) Hamley, I. W. *The Physics of Block Copolymers*; Oxford University Press: Oxford, 1998.
(5) Okamoto, S.; Saijo, K.; Hashimoto, T. *Macromolecules* **1994**, *27*, 5547−5555. Gupta, V. K.; Krishnamoorti, R.; Kornfield, J. A.; Smith, S. D. *Macromolecules* **1995**, *28*, 4464−4474.
(6) Tepe, T.; Hajduk, D. A.; Hillmyer, M. A.; Weimann, P. A.; Tirrell. M.; Bates, F. S.; Almdal, K.; Mortensen, K. *J. Rheol.* **1997**, *41*, 1147−1171.
(7) Vigild, M. E.; Chu, C.; Sugiyama, M.; Chaffin, K. A.; Bates, F. S. *Macromolecules* **2001**, *34*, 951−964.
(8) Hermel, T. J.; Wu, L.; Hahn, S. F.; Lodge, T. P.; Bates, F. S. *Macromolecules* **2002**, *35*, 4685−4689.
(9) Polis, D. L.; Smith, S. D.; Terrill, N. J.; Ryan, A. J.; Morse, D. C.; Winey, K. I. *Macromolecules* **1999**, *32*, 4668−4676.
(10) Zhang, Y.; Wiesner, U.; Yang, Y.; Pakula, T.; Spiess, H. W. *Macromolecules* **1996**, *29*, 5427−5431.
(11) Honeker, C. C.; Thomas, E. L.; Albalak, R. J.; Hajduk, D. A.; Gruner, S. M.; Capel, M. C. *Macromolecules* **2000**, *33*, 9395−9406.
(12) Keller, A.; Pedemonte, E.; Willmouth, F. M. *Nature (London)* **1970**, *225*, 538−539.
(13) Ryu, C. Y.; Lodge, T. P. *Macromolecules* **1999**, *32*, 7190−7201.
(14) Almdal, K.; Bates, F. S.; Mortensen, K. *J. Chem. Phys.* **1992**, *96*, 9122−9132.
(15) Förster, S.; Khandpur, A. K.; Zhao, J.; Bates, F. S.; Hamley, I. W.; Ryan, A. J.; Bras, W. *Macromolecules* **1994**, *27*, 6922−6935.
(16) Wang, C.-Y.; Lodge, T. P. *Macromolecules* **2002**, *35*, 6997−7006.
(17) Vigild, M. E.; Almdal, K.; Mortensen, K.; Hamley, I. W.; Fairclough, J. P. A.; Ryan, A. J. *Macromolecules* **1998**, *31*, 5702−5716.
(18) Almdal, K.; Koppi, K. A.; Bates, F. S. *Macromolecules* **1993**, *26*, 4058−4060.
(19) Diat, O.; Porte, G.; Berret, J.-F. *Phys. Rev. B* **1996**, *54*, 14869−14872.
(20) Hamley, I. W.; Pople, J. A.; Fairclough, J. P. A.; Terrill, N. J.; Ryan, A. J.; Booth, C.; Yu, G.-E.; Diat, O.; Almdal, K.; Mortensen, K.; Vigild, M. *J. Chem. Phys.* **1998**, *108*, 6929−6936.
(21) Bang, J.; Lodge, T. P.; Wang, X.; Brinker, K. L.; Burghardt, W. R. *Phys. Rev. Lett.* **2002**, *89*, 215505.
(22) McConnell, G. A.; Lin, M. Y.; Gast, A. P. *Macromolecules* **1995**, *28*, 6754−6764.
(23) Liu, T.; Burger, C.; Chu, B. *Prog. Polym. Sci.* **2003**, *28*, 5−26.
(24) Honeker, C. C.; Thomas, E. L. *Chem. Mater.* **1996**, *8*, 1702−1714.
(25) Zalusky, A. S.; Olayo-Valles, R.; Taylor, C. J.; Hillmyer, M. A. *J. Am. Chem. Soc.* **2001**, *123*, 1519−1520.
(26) Albalak, R. J.; Thomas, E. L. *J. Polym. Sci., Part B: Polym. Phys.* **1994**, *32*, 341−350.
(27) Albalak, R. J. *Polymer* **1994**, *35*, 4115−4119.
(28) Albalak, R. J.; Thomas, E. L.; Capel, M. S. *Polymer* **1997**, *38*, 3819−3825.
(29) Amundson, K.; Helfand, E.; Quan, X.; Smith, S. D. *Macromolecules* **1993**, *26*, 2698−2703.
(30) Böker, A.; Knoll, A.; Elbs, H.; Abetz, V.; Müller, A. H. E.; Krausch, G. *Macromolecules* **2002**, *35*, 1319−1325.
(31) Thurn-Albrecht, T.; DeRouchey, J.; Russell, T. P.; Jaeger, H. M. *Macromolecules* **2000**, *33*, 3250−3253.
(32) Bashir, Z.; Odell, J. A.; Keller, A. *J. Mater. Sci.* **1986**, *21*, 3993−4002.
(33) Schultz, J. M.; Hsiao, B. S.; Samon, J. M. *Polymer* **2000**, *41*, 8887−8895.

MA034417B